THE JOURNAL OF BIOLOGICAL CHEMISTRY
Vol. 273, No. 18, Issue of May 1, pp. 11189–11196, 1998
Printed in U.S.A.

Characterization of Recombinant and Brain Neuropsin, a Plasticity-related Serine Protease*

(Received for publication, May 16, 1997, and in revised form, February 10, 1998)

Chigusa Shimizu‡, Shigetaka Yoshida‡, Masao Shibata§, Keiko Kato‡, Yoshiharu Momota‡, Kazumasa Matsumoto‡, Takahiko Shiosaka¶, Ryosuke Midorikawa‡, Tomohiro Kamachi‡, Akiko Kawabe§, and Sadao Shiosaka‡‖

From the ‡Division of Structural Cell Biology, Nara Institute of Science and Technology, Nara Institute of Science and Technology, 8916-5 Takayama, Ikoma, Nara 630-0101, the §Medical and Biological Laboratories Company, Limited, 1063-103 Ohara, Ina, Nagano 396, and the ¶Department of Medical Laboratory Technology, Ehime College of Health Science, 543 Takaoda, Iyo, Ehime 791-21, Japan

Activity-dependent changes in neuropsin gene expression in the hippocampus implies an involvement of neuropsin in neural plasticity. Since the deduced amino acid sequence of the gene contained the complete triplet (His-Asp-Ser) of the serine protease domain, the protein was postulated to have proteolytic activity. Recombinant full-length neuropsin produced in the baculovirus/insect cell system was enzymatically inactive but was readily converted to active enzyme by endoprotease processing. The activational processing of prototype neuropsin involved the specific cleavage of the Lys^{32}-Ile^{33} bond near its N terminus. Native neuropsin that was purified with a purity of 1,100-fold from mouse brain had enzymatic characteristics identical to those of active-type recombinant neuropsin. Both brain and recombinant neuropsin had amidolytic activities cleaving Arg-*X* and Lys-*X* bonds in the synthetic chromogenic substrates, and the highest specific activity was found against Boc-Val-Pro-Arg-4-methylcoumaryl-7-amide. The active-type recombinant neuropsin effectively cleaved fibronectin, an extracellular matrix protein. Taken together, these results indicate that this protease, which is enzymatically novel, has significant limbic effects by changing the extracellular matrix environment.

Some proteases have been suggested to be related to neural cell dynamics in such processes as cell death, migration, cell-to-cell adhesion and de-adhesion, process elongation, pathfinding, and axonal rearrangement (1–5). These phenomena have been investigated by supplying known proteases involved in blood coagulation, fibrinolysis, or digestion to neural cell cultures. However, the observations that the proteases are mainly localized in and released from non-neural cells do not support all of such neural effects (5–7). Thus, we postulated that neurons themselves may produce and release their own proteases to participate in the neural cell dynamics described above.

Neuropsin (NP)[1] was cloned from the mouse brain and was shown to be localized in mouse hippocampal pyramidal neurons (8). These results and the observation that its mRNA showed marked activity-dependent changes caused by plasticity-inducible stimuli are suggestive of some neural effects in limbic plasticity (8, 9). However, it is still not known whether NP protein has enzyme activity as suggested by the deduced amino acid sequence (8). We postulated that the enzyme activity might be a molecular basis for the physiological responses induced by various stimuli. Therefore, in the present study, we examined whether recombinant NP (r-NP) and brain NP had proteolytic activity against synthetic and natural substrates.

EXPERIMENTAL PROCEDURES

Materials—Mono S, Sepharose 2B, CNBr-activated Sepharose 4B and CL-6B, Superdex-75HR, Superose 12, Resource S, and Protein G-Sepharose were from Amersham Pharmacia Biotech. Silver staining kits were from Bio-Rad. Diisopropyl fluorophosphate (DFP), benzamidine, bestatin, soybean trypsin inhibitor, human plasma thrombin (EC 3.4.4.13), and TNM-FH insect cell medium were purchased from Sigma. [1,3-^{3}H]DFP was from NEN Life Science Products. D-Pro-Phe-Arg-pNA, D-Val-Leu-Arg-pNA, and D-Val-Leu-Lys-pNA were from Daiichi Pure Chemicals (Tokyo, Japan). *N*-Bz-DL-Lys-pNA, dimethyl sulfoxide, aprotinin, protease 1 (*Achromobacter lyticus,* EC 3.4.21.50), trypsin (EC 3.4.21.4), and polyethylene glycol 20,000 were from Wako Pure Chemical Inc. (Osaka, Japan). Bz-Tyr-pNA, L-Leu-pNA, Bz-L-Arg-pNA, Boc-Val-Pro-Arg-MCA, Z-Pro-Phe-Arg-MCA, Boc-Glu-Lys-Lys-MCA, Pyroglutamyl-Gly-Arg-MCA, glutaryl-Gly-Arg-MCA, Boc-Phe-Ser-Arg-MCA, succinyl-Leu-Leu-Val-Tyr-MCA, Boc-Asp-Pro-Arg-MCA, Boc-Glu-Gly-Arg-MCA, Boc-Leu-Arg-Arg-MCA, Boc-Leu-Thr-Arg-MCA, Boc-Gly-Arg-Arg-MCA, Boc-Ala-Gly-Pro-Arg-MCA, *N*-(L-3-*trans*-carboxyoxiran-2-carbonyl)-L-leucyl-agmatin (E-64), pepstatin A, leupeptin, chymostatin, and antipain were from Peptide Institute Inc. (Osaka, Japan). Bicinchoninic acid protein assay kit was from Pierce. pVL1392 transfer vector was from Invitrogen. BaculoGold transfection kit was from PharMingen (San Diego, CA). Serum-free medium for insect cells, SF-900II, and human plasma fibronectin were from Life Technologies, Inc. Fetal bovine serum and (4-amidinophenyl)methanesulfonyl 1-fluoride were from Boehringer Mannheim (Germany). Horseradish peroxidase-labeled goat anti-rat IgG was purchased from Cappel. All other reagents used were of analytical grade.

Cloning of Full-length NP cDNA into Baculovirus—The 866-base pair NP3 cDNA was subcloned into the *Not*I site of the pVL1392 transfer vector to create plasmid pVL1392/NP3 (Fig. 1) (8). Plasmid DNA was transferred into the AcNPV genome by homologous recombination so that Sf21 cells were transfected with transfer vector and AcNPV DNA. The presence of the NP3 cDNA was confirmed by dot blot

* This work was supported in part by a Grant-in-Aid for Scientific Research on Priority Areas from the Ministry of Education, Science, Sports and Culture of Japan. The costs of publication of this article were defrayed in part by the payment of page charges. This article must therefore be hereby marked "*advertisement*" in accordance with 18 U.S.C. Section 1734 solely to indicate this fact.

‖ To whom correspondence should be addressed: Division of Structural Cell Biology, Nara Institute of Science and Technology, 8916-5 Takayama, Ikoma, Nara 630-0101, Japan. Tel.: 81-74372-5410; Fax: 81-74372-5419; E-mail: sshiosak@bs.aist-nara.ac.jp

[1] The abbreviations used are: NP, neuropsin; r, recombinant; DFP, diisopropyl fluorophosphate; pNA, *p*-nitroanilide; MCA, 4-methylcoumaryl-7-amide; Bz, benzyl; Boc, *t*-butyloxycarbonyl; Z, benzyloxycarbonyl; E-64, *N*-(L-3-*trans*-carboxyoxiran-2-carbonyl)-L-leucyl-agmatin; PAGE, polyacrylamide gel electrophoresis; tPA, tissue-type plasminogen activator; MALDI-TOFMS, matrix-assisted laser desorption/ionization time-of-flight mass spectrometry; FnI, fibronectin type I.

hybridization. Positive virus clones were harvested from the culture medium, and the DNA was characterized by Southern blotting.

Production of r-NP in Insect Cells—Sf21 insect cells were grown at 27 °C in TNM-FH medium containing 10% heat-inactivated fetal calf serum to a density of 7×10^6/75-cm^2 tissue culture flask. For infection, cells were centrifuged for 5 min at 500 × *g* at room temperature and resuspended in serum-free SF900II medium. Cells at a density of 1×10^6 cells/ml were infected with recombinant baculovirus at a multiplicity of infection of 1. Three to five days postinfection, the incubation medium was harvested by removing the cells by centrifugation at 500 × *g* for 10 min at 4 °C. The supernatant was clarified by centrifugation at 4 °C, 25,000 × *g*, for 1 h and dialyzed against 10 mM HEPES buffer (pH 7.4) for 2 days. The supernatant was then concentrated using Spectrapore Membranes (M_r 3500) against polyethylene glycol 20,000 at 4 °C and dialyzed against 10 mM HEPES buffer (pH 7.4). This solution was subjected to anion exchange chromatography using a 6-ml column of Resource S. Bound protein was eluted with a linear gradient of 0 to 1 M NaCl in 50 min at a flow rate of 2 ml/min; NP was eluted at 0.44–0.58 M NaCl. For further purification, the protein was concentrated by Centricon 10 (Amicon), dialyzed against 50 mM HEPES, 0.15 M NaCl (pH 7.4), and gel-filtrated with a 10 × 300-mm column of Superdex 75 HR. The recombinant protein samples were then applied to SDS-PAGE, followed by silver staining under both reducing and non-reducing conditions as described below. The expressed recombinant protein had no or only low amidolytic activity, and this was assumed to be pro-NP (r-pro-NP) (Table I).

Production of Monoclonal Antibodies against r-pro-NP—Wistar rats were immunized by intraperitoneal injection of 50 μg of purified r-pro-NP emulsified with Freund's adjuvant several times. After titration of rat serum by Western blotting, the rats were intraperitoneally boosted with 50 μg of the r-pro-NP on 2 days before cell fusion. Isolated spleen cells from the immunized rats were fused with Y3Ag.1.2.3 rat myeloma cells (10). After selection in hypoxanthine/aminopterin/thymidine medium, the supernatants of hybridomas were screened for production of specific antibodies to r-pro-NP by Western blotting and enzyme-linked immunosorbent assay using microplates coated with r-pro-NP. Positive clones were used for the production of ascites in pristane-primed nude rats (F344/N Jcl). We screened for the clone producing the most specific monoclonal antibody with the highest titer. The monoclonal antibodies (mAbF12 and mAbB5) were purified from ascites by affinity chromatography on protein G-Sepharose. Neither antibody showed cross-reactivity against serine proteases localized in the brain such as α-thrombin, trypsin, kallikrein, tissue, or urokinase plasminogen activator (11).

Electrophoresis and Western Blotting—SDS-PAGE was carried out using 12.5% gels (12), followed by silver staining (13). The electrophoresed protein was transferred from the gels onto nitrocellulose membranes which were then incubated overnight with anti-NP monoclonal antibody diluted with 0.1 M Tris-HCl buffer (pH 7.5) containing 1% Tween 20 and 0.15 M NaCl at 4 °C. After washing with the same buffer, the blotted membranes were incubated with horseradish peroxidase-labeled goat anti-rat IgG diluted with 0.1 M Tris-HCl buffer (pH 7.5) containing 1% Tween 20, 0.15 M NaCl, and 5% bovine serum albumin at room temperature for 1 h. Immunoreactivity was visualized with 0.04% 3,3′-diaminobenzidine and 1.2% NH_3NiSO_4 in 50 mM Tris-HCl buffer (pH 7.5) containing 0.04% H_2O_2.

Activation of r-Pro-NP by Endoproteases—Protease 1 (EC 3.4.21.50) and trypsin (EC 3.4.21.4) were used for activational processing of r-pro-NP, the enzymatically inactive form. Protease 1 more effectively processed r-pro-NP than trypsin, converting it to the active form, and was thus used in the subsequent experiments. Protease 1 was immobilized on CNBr-activated Sepharose 4B prior to use and was used to convert r-pro-NP to r-NP. Briefly, Sepharose 4B was washed several times with coupling buffer (0.5 M NaCl in 0.1 M $NaHCO_3$ (pH 8.3)). Ten mg of protease 1 dissolved in the coupling buffer was added to 1 g of the gel. After incubation in 0.2 M glycine (pH 8.0) to block free CNBr residues, the Sepharose 4B-immobilized protease 1 was washed several times with either 0.5 M NaCl in 0.1 M Tris-HCl (pH 8.0) or 0.5 M NaCl in 0.1 M acetate buffer (pH 4.0). The immobilized protease 1 was stored in 0.1 M Tris-HCl buffer (pH. 8.0) containing 0.5 M NaCl. In special cases, protease 1 which was not immobilized on the gel was also used (*cf.* Fig. 2).

N-terminal Sequencing of r-NP—N-terminal amino acid sequencing of r-NP was performed with an ABI 477 pulsed liquid sequencer using standard sequencing chemistry. Purified samples were spotted onto Immobilon membranes (Millipore) 5 mm in diameter and were put on top of a UF membrane. The Immobilon membranes with bound protein were then washed with 50% methanol and sequenced by Edman degradation.

Time-of-flight Mass Spectrometry—Matrix-assisted laser desorption/ionization time-of-flight mass spectrometry (MALDI-TOFMS) was performed using PerSeptive Biosystems (Framingham, MA) Voyager Elite. The accelerating voltage of the ion source was 25 kV. Data were acquired with a 20 MHz digitizer. The matrix used for r-NP and r-pro-NP was sinapinic acid. The matrix material was dissolved in aqueous CH_3CN (33%, v/v) to give a saturated solution. Ten pmol of r-NP or r-pro-NP was mixed with the matrix prior to loading on the plate. Bovine serum albumin and 2-thioredoxin were used as molecular mass standards.

Platelet Aggregation Assay—Platelet-rich plasma was obtained from human blood from a volunteer donor containing 3.5% sodium citrate. Platelets were isolated by gel filtration with a Sepharose 2B column in HEPES-Tyrode's buffer. Aggregation was performed at 37 °C with 200 μl of 2×10^8 platelets/ml containing 150 μg of fibrinogen in an aggregometer (Aggretec model TE-500 ERMER). Varying concentrations of thrombin (0.1 and 0.5 units) or r-NP (0.1, 1, and 2 units) were added to the aggregometer tube.

Cleavage of Fibronectin by r-NP—Aliquots of 4 μg of human plasma fibronectin were incubated with 0.4 μg of r-pro-NP or r-NP in 20 μl of 0.2 M Tris-HCl buffer (pH 8.0). Reaction was performed at 37 °C for 1, 2, 4, 8, and 16 h and was then terminated by boiling for 3 min with loading buffer (5 μl of 60 mM Tris-HCl (pH. 6.8) containing 2% SDS, 7% glycerol, and 0.05% bromphenol blue). Samples were electrophoresed on 6.25% polyacrylamide gels, followed by Coomassie Blue staining.

To analyze cleavage sites of fibronectin by r-NP, the digestion products were electrophoresed and transferred onto Immobilon membranes. The transferred bands on membranes corresponding to degraded fibronectin were cut out and subjected to N-terminal sequencing as described above.

Immunoaffinity Purification of Mouse Brain NP—Affinity gel was prepared using the monoclonal antibody produced as described above. Six mg of mAbB5 was dialyzed against 0.1 M carbonate buffer (pH 9.0) overnight. CNBr-activated Sepharose CL-6B was activated and coupled to mAbB5.

Adult BALB/c mouse brains (10 g) were homogenized with 10 mM HEPES-NaOH (pH 7.4), 1% Triton X-100 and centrifuged at 10,000 × *g* for 1 h. The supernatant was applied to a mAbB5-coupled affinity column equilibrated with 10 mM sodium phosphate buffer (pH 7.4) containing 0.3 M NaCl. Elution was performed with 0.17 M glycine HCl (pH 2.3) into tubes containing 1 M Tris-HCl (pH 9.0), for neutralization. Fractions were analyzed by 12.5% SDS-PAGE-silver staining by Western blotting and by assay for amidolytic activity (described below).

Measurement of Amidolytic Activity of r-NP and Brain NP—Amidolytic activities of r-NP and brain NP were monitored by release of MCA or pNA from the synthetic substrates listed above. Assay mixtures containing chromogenic substrates at 100 μM and 45 mM Tris-HCl buffer (pH 8.0) and 10 μl of r-NP or brain NP samples were incubated at 37 °C for 30 min. Released MCA and pNA were measured with a Hitachi fluorescent colorimeter equipped with 370-nm excitation and 460-nm absorption filters, and with a Bio-Rad microplate reader with a 405-nm absorbance filter, respectively.

Kinetic analysis of r-NP and brain NP was performed by incubation of 100 ng of enzyme and increasing concentrations of amidolytic substrates at 37 °C for 30 min. The kinetic parameters of amidolysis were determined using a double-reciprocal Lineweaver-Burk plot for the rate of release of MCA *versus* substrate.

Protein concentration was assayed by bicinchoninic acid protein assay using bovine serum albumin as a standard (14).

DFP Affinity Labeling of r-NP and Brain NP—r-NP and brain NP in 10 mM HEPES buffer (pH 7.4) were mixed with [^{3}H]DFP (222 Bq/mmol) and incubated at 37 °C for 10 h. Nonspecific binding of [^{3}H]DFP was removed by addition of 2 μl of cold 5.4 M DFP and 10 μl of bovine serum albumin (1 mg/ml) and washing with ice-cold acetone (100%). The samples were precipitated at 12,000 × *g* for 15 min and subjected to SDS-PAGE. The polyacrylamide gel was fixed with distilled water: isopropyl alcohol:acetate (65:25:10) and exposed to Fuji x-ray film for 3 days.

Subcellular Fractionation of Mouse Hippocampus Homogenate—All fractionation steps in Fig. 7*A* were carried out at 4 °C. The tissue extraction procedure followed that of Yen *et al.* (15). The hippocampi and the cerebrums from 12 ddY mice were homogenized with 12 ml of ice-cold Tris-buffered saline (20 mM Tris-HCl (pH 7.4), 0.15 M NaCl), incubated for 15 min, and then centrifuged at 10,000 × *g* for 10 min. The supernatant was referred to as 0.15 M NaCl-soluble fraction (A). The pellet was rehomogenized with an equal volume of 20 mM Tris-HCl

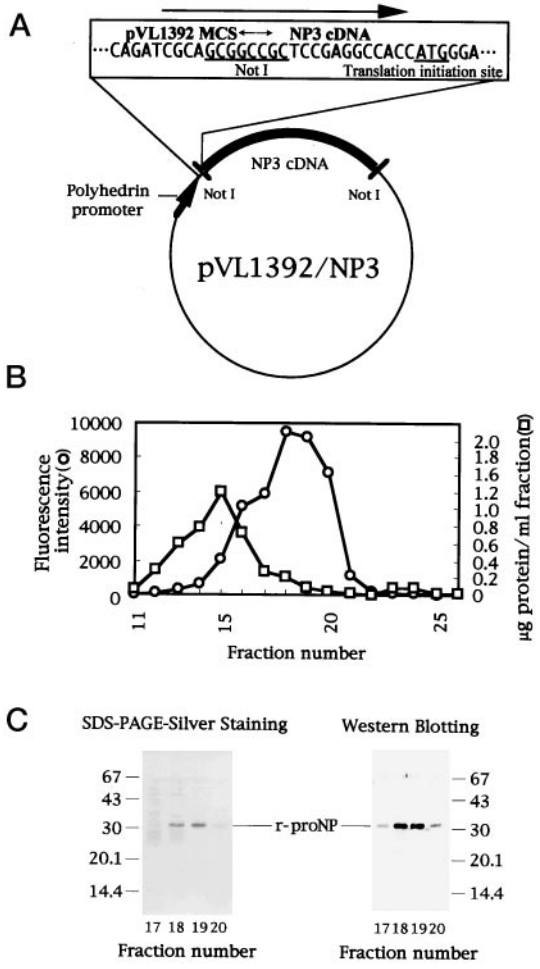

FIG. 1. **Construction of the pVL1392/NP3 plasmid and purification of r-pro-NP.** *A*, an 866-base pair *Not*I restriction fragment of NP3 cDNA containing the entire open reading frame of mouse pro-NP was inserted into the unique *Not*I cloning site under the control of the strong polyhedrin promoter in the vector pVL1392. The sequence at the insertion sites is highlighted to indicate the detailed positioning of the coding region relative to the polyhedrin promoter and the multicloning site of pVL1392. *B*, amidolytic activity of the eluate from Superdex 75HR gel filtration for purification of r-pro-NP. Fractions (0.5 ml) were collected at a flow rate of 0.5 ml/min. Enzyme activities were measured using aliquots of each fraction (11–26) after activation of r-NP (see "Experimental Procedures"). ○, fluorescence intensity of MCA released from Boc-Val-Pro-Arg-MCA (λ_{em} 370 nm and λ_{ex} 460 nm); □, protein content. *C*, SDS-PAGE and silver staining showed a single band of r-pro-NP in *fraction 19* (*left*). The fractions were characterized by immunodetection using anti-NP antibody (*right*). Purified r-pro-NP migrated at a position corresponding to approximately 32 kDa. Molecular masses of standards (kDa) are indicated in the *left* and *right* margins.

(pH 7.4), 2% Triton X-100, incubated for 10 min, and then ultracentrifuged at 102,000 × *g* for 10 min. The supernatant was referred to as Triton X-100 soluble fraction (B). The pellet was further rehomogenized with an equal volume of 20 mM Tris-HCl (pH 7.4), 1% Triton X-100, incubated for 10 min, and ultracentrifuged at 208,000 × *g* for 10 min. The supernatant was referred to as Triton X-100 soluble fraction (C). The pellet was further rehomogenized with an equal volume of 20 mM Tris-HCl (pH 7.4), 0.5 M NaCl, incubated for 10 min, and then ultracentrifuged at 383,000 × *g* for 10 min. The supernatant was referred to as cytoskeleton-rich fraction (D). Each fraction was then immunoprecipitated with anti-NP antibody (mAbB5) and immunoblotted with anti-NP polyclonal rabbit antiserum. SDS-PAGE was performed as described above.

RESULTS

Production, Purification, and Activation of r-pro-NP—The full murine NP sequence was subcloned into the *Not*I site of the pVL1392 transfer vector (Fig. 1*A*) (8). By SDS-PAGE and silver staining, a major 32-kDa product was detected in the medium derived from infected cells (Fig. 1, *B* and *C*) but not from uninfected cells (data not shown). The 32-kDa protein was immunoreactive with anti-NP monoclonal antibody (mAbB5) on Western blotting, and this band was therefore presumed to correspond to recombinant NP protein. However, conditioned media from infected and non-infected insect cells both lacked amidolytic activity for various synthetic substrates (Table I). Therefore, we speculated that the 32-kDa protein is a non-active prototype NP protein (r-pro-NP). Conditioned medium from infected insect cells showed high amidolytic activity following the endoprotease processing (fluorescence intensity was 5130 per 1 μl of medium; see details below; see also Figs. 1*B* and 2 and Table I), whereas the medium from non-infected cells still showed very low amidolytic activity even after endoprotease treatment (60.3 fluorescence intensity per 1 μl of medium).

TABLE I
Enzyme activities of r-proNP, r-NP, and brain NP toward various synthetic substrates

Enzyme activities were determined as described under "Experimental Procedures" and are expressed as specific activities. Percentage of activity toward Boc-Val-Pro-Arg-MCA is shown in parentheses in r-NP and brain NP.

Substrate	Specific activity		
	r-proNP	r-NP	Brain NP
	Units[a]/mg protein	Units/mg protein	Units/mg protein
		%	%
Boc-Val-Pro Arg-MCA	0.01	6.26 (100)	1.23 (100)
Boc-Phe-Ser-Arg-MCA	0	4.88 (78)	0.50 (41)
D-Val-Leu-Arg-pNA	0	1.75 (28)	0.38 (31)
Boc-Ala-Gly-Pro-Arg-MCA	—[b]	1.7 (27)	—
Boc-Glt[c]-Gly-Arg-MCA	—	1.48 (24)	0.30 (24)
Boc-Asp-Pro-Arg-MCA	—	1.41 (22)	—
Boc-Glu-Gly-Arg-MCA	—	1.33 (21)	—
D-Val-Leu-Lys-pNA		1.27 (20)	0.29 (24)
Boc-Pyr[d]-Gly-Arg-MCA	—	1.27 (20)	0.34 (28)
Boc-Glu-Lys-Lys-MCA	—	1.21 (19)	0.27 (22)
Boc-Leu-Thr-Arg-MCA	—	1.07 (17)	—
Boc-Leu-Arg-Arg-MCA		1.01 (16)	—
Z-Pro-Phe-Arg-pNA	—	0.79 (13)	—
Boc-Gly Arg-Arg-MCA	—	0.71 (11)	—
Suc-Leu-Leu-Val-Tyr MCA	—	0 (0)	0 (0)
Z-Phe-Arg-MCA	—	0 (0)	0 (0)
Bz-Tyr-pNA	—	0 (0)	0 (0)
Bz-L-Arg pNA	—	0 (0)	0 (0)
Bz-L-Leu-pNA	—	0 (0)	0 (0)
N-Bz-DL-Lys-pNA	—	0 (0)	0 (0)

[a] One unit of activity was defined as that required to hydrolyze 1 μmol/min chromogen.
[b] —, not tested.
[c] Glt, glutaryl.
[d] Pyr, Pyroglutamyl.

The culture medium derived from infected insect cells was subjected to anion exchange chromatography in one step to purify r-pro-NP. One major peak of protein eluted by a linear NaCl gradient was collected. As the fractions contained minor cell products, they were pooled and concentrated before being applied to gel chromatography in the second step to remove the minor components. The fractions eluted from gel chromatography were used for assay of amidolytic activity after activation by gel-immobilized protease 1 (Fig. 1*B*, *cf.* Fig. 2). A single peak of cleavage activity of Boc-Val-Pro-Arg-MCA was observed in *fractions 17–20* (Fig. 1*B*). To check the purity, SDS-PAGE of the fractions was performed, and proteins were transferred onto nitrocellulose membranes. Fraction 19 showed a single band by SDS-PAGE followed by silver staining and Western blotting with mAbB5 and was thus used as purified r-pro-NP (Fig. 1*C*).

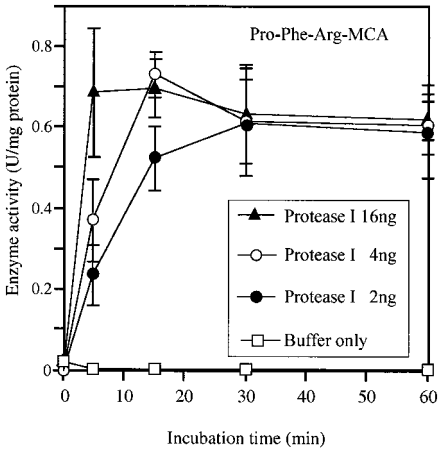

FIG. 2. **Activational processing of r-pro-NP by endoprotease.** The *horizontal axis* indicates the incubation time of r-pro-NP with various amounts of protease I. Enzyme activities were measured with Pro-Phe-Arg-MCA as a substrate, because no amidolytic activity was identified on this substrate by protease 1 itself. The reaction of r-NP was started by addition of the substrate. The *error bars* indicate S.D. One unit of activity was defined as that required to hydrolyze 1 μmol/min chromogen.

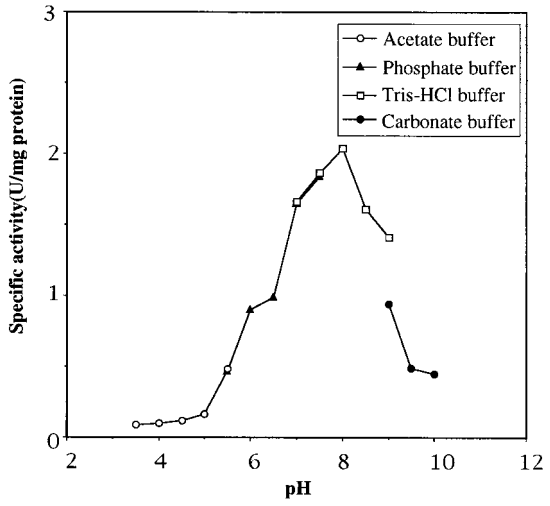

FIG. 3. **Effects of pH on activity of r-NP.** Enzyme activity of r-NP was measured by addition of Boc-Val-Pro-Arg-MCA as a substrate. The buffers used were acetate buffer, pH 3.5–5.5 (○); phosphate buffer, pH 5.5–7.5 (▲); Tris-HCl buffer (pH 7.0–9.0) (□); and carbonate buffer, pH 9.0–10.0 (●) at a final concentration of 0.1 M.

Endoprotease treatment of r-pro-NP induced rapid induction of amidolytic activity by conversion to r-NP (Fig. 2). The enzyme activity in this experiment was observed using Z-Pro-Phe-Arg-MCA, whereas it was cleaved less effectively than Boc-Val-Pro-Arg-MCA because it was not cleaved by protease 1 itself (Table I). To examine the time course of the induction of activity, various concentrations of protease 1 were incubated with purified r-pro-NP. The r-pro-NP was processed in a dose-dependent manner after 5 min of incubation with protease 1 (Fig. 2). Longer incubation resulted in the enzyme activity reaching a plateau with almost the same activity at 2, 4, and 16 ng of protease 1 (Fig. 2). No induction of the enzyme activity was observed when protease 1 was omitted (Fig. 2, *open squares*). Enzyme activity of r-NP was characterized using this activated recombinant protein produced by endoprotease processing of r-pro-NP. The effects of pH on r-NP amidolytic activity were examined using four different buffers as follows: acetate (pH 3.5–5.5), phosphate (pH 5.5–7.5), Tris-HCl (pH 7.0–9.0), and carbonate buffer (pH 9.0–10.0). As shown in Fig. 3, the pH optimum for the enzyme activity was around pH 8.0.

To confirm that r-pro-NP is a zymogen of r-NP, we performed N-terminal amino acid sequencing of both r-pro-NP and r-NP. The sequenced N-terminal peptide of r-NP was comprised of 7 amino acids and started at Ile^{33}, 33 amino acids downstream of the deduced amino acid sequence of the NP3 cDNA (data not shown). On the other hand, the N terminus of r-pro-NP was blocked and not sequenced. To identify the N-terminal amino acid of r-pro-NP, the difference of molecular weight between r-NP and r-pro-NP was analyzed by matrix-assisted laser/desorption ionization time-of-flight mass spectrometry (MALDI-TOFMS). MALDI-TOFMS revealed that the molecular masses of r-pro-NP and r-NP were 26.613 and 26.229 kDa, respectively, and thus r-NP was 384 daltons less than r-pro-NP. This difference was suggested to be caused by an N-terminal peptide of r-pro-NP composed of 4 amino acid residues, Gln^{29}-Lys^{32} (calculated M_r = 400). Some unknown modification(s), probably cyclization, of the N-terminal Gln of r-pro-NP might have been responsible for the inability to determine its N-terminal sequence. Hydrophobicity plot analysis of the deduced amino acid sequence of the NP3 cDNA showed that the peptide from Met^{1}-Ala^{28} is highly hydrophobic (16), and this was postulated to be the signal sequence. Therefore, we concluded that secreted r-pro-NP from infected insect cells undergoes activational processing at the Lys^{32}-Ile^{33} bond as shown in the model (Fig. 4).

As described above, the molecular mass of r-pro-NP was determined to be 26.6 kDa by MALDI-TOFMS analysis. This is in good agreement with the calculated molecular mass (25.5 kDa) from the amino acid content deduced from the cDNA (8). The molecular mass was estimated by SDS-PAGE under reducing and non-reducing conditions as 32 (Fig. 1*C*) and 26 kDa (Fig. 7*B*), respectively, and by Superose 12 size exclusion chromatography at 29 kDa, suggesting that the enzyme exists as a monomer.

Substrates and Inhibitors of r-NP—Table I shows amidolytic activities of r-pro-NP and r-NP on various synthetic substrates. The highest amidolytic activity was observed toward Boc-Val-Pro-Arg-MCA, a substrate of α-thrombin. Boc-Phe-Ser-Arg-MCA, which is a substrate of trypsin, was also a good substrate for r-NP. The effects of various protease inhibitors on amidolytic activity of r-NP are shown in Table II. The enzyme activities measured were strongly inhibited by low molecular weight protease inhibitors that bind to His and Ser residues in the active centers of serine proteases. DFP, leupeptin, and (4-amidinophenyl)methanesulfonyl 1-fluoride belong to this group. Inhibition was also seen with benzamidine and antipain. Both pepstatin A, an aspartic protease inhibitor, and E-64, a cysteine protease inhibitor, had no or only slight effects on r-NP activity. In addition, the divalent cations Ca^{2+} and Mg^{2+} and metal ion chelators had little effect on r-NP activity. Thus, NP was categorized as a serine protease and not an aspartic, cysteine, or metalloprotease.

Classified inhibitors were applied to define the r-NP activity. Specific low molecular weight inhibitors of chymotrypsin and trypsin, chymostatin and aprotinin markedly inhibited the amidolytic activity of r-NP. However, high molecular weight inhibitors of serine proteases did not significantly inhibit the enzyme activity (Table II). Hence, NP has a similar catalytic center to trypsin and chymotrypsin, but the substrate specificity due to the structure of the active site might be very different from those of these enzymes (see "Discussion").

No Platelet Aggregation Activity of r-NP—As the r-NP favorably cleaved Boc-Val-Pro-Arg-MCA, a synthetic substrate of α-thrombin, thrombin-like blood coagulation activity was analyzed. Although 0.1 and 0.5 units of thrombin, used as a positive control, had strong platelet aggregation activity, no activ-

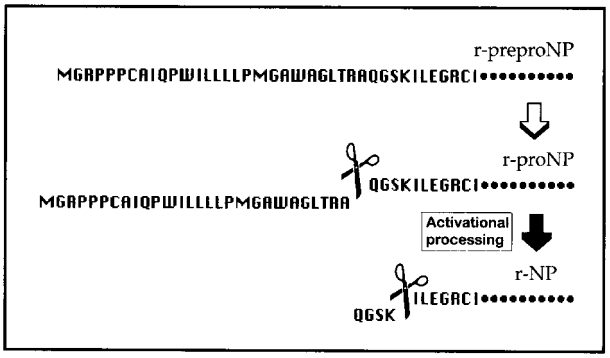

FIG. 4. **Model of activational processing of r-NP.** Starts of r-pro-NP (Gln^{29}) and r-NP (Ile^{33}) were revealed by MALDI-TOFMS and N-terminal sequencing analyses, respectively. N-terminal signal sequence (Met^{1}-Ala^{28}) of recombinant protein that was translated from the entire open reading frame of the NP3 cDNA (8) was removed (r-pro-NP) and secreted from insect cells as an enzymatically inactive zymogen (*open arrow*). The r-pro-NP readily underwent activational processing by protease 1, a lysine-specific endopeptidase, to generate the enzymatically active form (r-NP) by removal of Gln^{29}-Lys^{32} (*filled arrow*).

TABLE II
Effects of inhibitors on protease activity of r-NP

Inhibitor	Concentration	Inhibition
	mM	%
Low molecular weight inhibitors		
DFP	0.01	5
	0.1	16
	1	38
	10	100
Leupeptin	0.01	75
	0.1	100
APMSF[α]	0.1	0
	0.3	19
	1	61
	3	87
Benzamidine	0.1	10
	1	56
Antipain	0.01	75
	0.1	95
Chymostatin	0.01	45
	0.1	80
	10	85
Aprotinin	0.01	5
	0.1	65
	10	84
Pepstatin A	0.01	0
	0.1	0
E-64	0.01	0
	0.1	15
High molecular weight inhibitors		
Human α1-antitrypsin	2	14
	10	20
Human α1-antichymotrypsin	0.4	7
	2	16
Trypsin inhibitor	0.01 (mg/ml)	0
	0.1	0

[α] APMSF, (4-amidinophenyl)methanesulfonyl 1-fluoride.

ity was found in r-NP at any concentration tested (0.1, 1, and 2 units; data not shown). These results suggested that r-NP does not process thrombin receptor protein (present results and see Refs. 17 and 18).

Degradation of Fibronectin by r-NP, but Not by r-pro-NP—No or only weak proteolytic activities of r-NP against gelatin and collagen types I, III, IV, and VI were detected by zymography (data not shown). Strong proteolytic activity of r-NP was found against fibronectin, an extracellular matrix protein, which is widely distributed in the nervous system. Human plasma fibronectin is composed mainly of a 440-kDa dimer with lesser but variable amounts of lower molecular

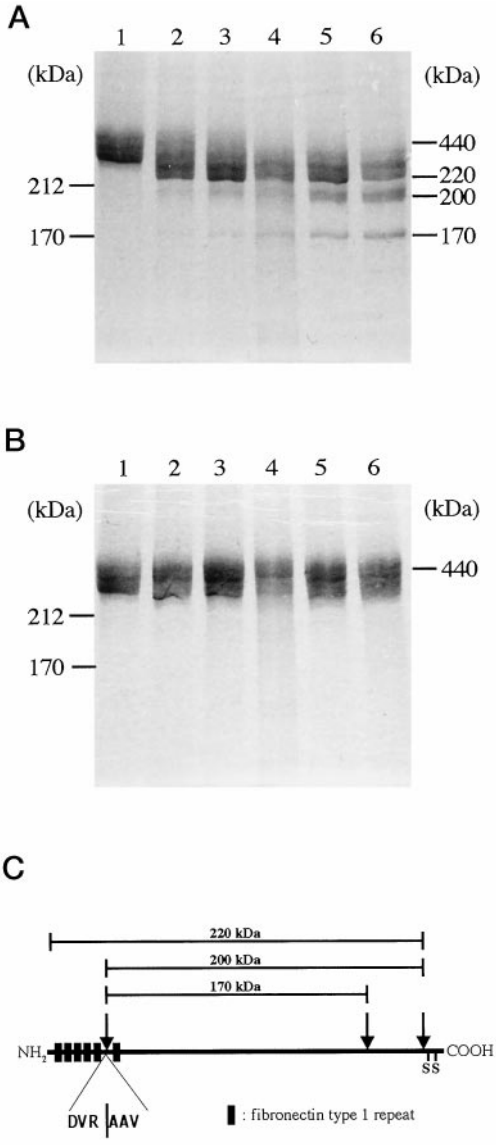

FIG. 5. **Cleavage of fibronectin by r-NP but not by r-pro-NP.** Time courses of fibronectin digestion by r-NP (*A*), and fibronectin digestion by r-pro-NP (*B*). Human plasma fibronectin (4 μg) was incubated in the absence (*lane 1*) or presence (*lanes 2–6*) of r-NP or r-pro-NP at 37 °C. Samples were electrophoresed on a 6.25% polyacrylamide gel under non-reducing conditions and analyzed by staining with Coomassie Blue. Molecular masses of standards (kDa) are indicated in the *left margin*. Fibronectin alone (*lane 1*) or fibronectin which was incubated with 0.4 μg of r-NP or r-pro-NP for 1 h (*lane 2*), 2 h (*lane 3*), 4 h (*lane 4*), 8 h (*lane 5*), and 16 h (*lane 6*) were electrophoresed. Fibronectin was gradually cleaved into small fragments in *A* (r-NP), whereas no cleavage was observed in *B* (r-pro-NP). *C*, a diagram indicating the cleavage sites of fibronectin by r-NP. The cleavage site between fifth and sixth fibronectin type 1 repeats of N terminus (Arg-Ala) were shown.

weight forms, when analyzed under non-reducing conditions (*lane 1* in Fig. 5, *A* and *B*). Upon incubation with r-NP, the molecular mass of fibronectin gradually decreased from the 440-kDa dimer to 220-, 200-, and 170-kDa monomers (Fig. 5*A, lanes 2–6*), although no degradation of fibronectin was induced by r-pro-NP (Fig. 5*B, lanes 2–6*). The 220-kDa fragment, which is the monomeric form of fibronectin (19), appeared initially, followed by the 200- and 170-kDa degradation products in a time-dependent manner. Furie and Rifkin (20) demonstrated that the interchain disulfide bridges of the dimerized fibronectin are present very close to the C terminus. Together with this finding, our results indicate that r-NP-mediated cleavage might occur initially near the C-terminal region.

TABLE III
Purification of NP from mouse brain

Procedure	Volume	Protein	Total activity	Specific activity	Purity (integers)	Yield
	ml	*mg*	*units*[a]	*units*[a]*/mg protein*		*%*
Brain homogenate	19.7	220	0.11	0.0005	1	100
Immunoaffinity chromatography	0.6	0.14	0.08	0.55	1100	72.7

[a] One unit of activity was defined as that required to hydrolyze 1 μmol/min chromogen.

Next, we performed N-terminal amino acid sequencing of the 200- and 170-kDa degradation products and found that these degradation products started at the same site, Ala^{291}. Therefore, r-NP cleaves specific sites of fibronectin as follows: 1) the C terminus, and 2) a site between the fifth and sixth fibronectin type I repeats (FnI). The five FnI repeats in the N terminus are lost following r-NP treatment for 2 h or more (Fig. 5, *A* and *C*). No further degradation was observed with incubation up to 6 h (Fig. 5*A*). Thus, the degradation step of fibronectin was very specific and might be important for physiology of cells because the N-terminal five FnI repeats contain important functional sites (Fig. 5*C*, Ref. 21; see also "Discussion").

Partial Purification of Mouse Brain NP—We focused on enzyme characterization of native NP. For this purpose, brain NP from mouse brain homogenate was partially purified (Table III). One-step immunoaffinity chromatography after detergent solubilization of brain lysate resulted in purification with a 1,100-fold purity and a 72.7% recovery with a major band on SDS-PAGE visualized by silver staining (Fig. 6*A*, *asterisks* in fractions 3 and 4; Table III). The amidolytic activity measured with Boc-Val-Pro-Arg-MCA as a substrate was eluted in fractions 3 and 4 (Fig. 6*B*). Western blotting analysis showed a dense band of 32 kDa in fractions 3 and 4 (Fig. 6*C*). A faint band of 30 kDa in fractions 3 was considered to be a degradation product of NP because it showed immunoreactivity. SDS-PAGE of ^{3}H-labeled DFP-bound protein originating from fractions 3 and 4 followed by autoradiography showed a single band of approximately 32 kDa (Fig. 6*D*). Therefore, the 32-kDa protein was considered to be brain active-type NP. In addition, an approximately 50-kDa minor component visualized by silver staining, but which was not immunoreactive on Western blotting and did not bind [^{3}H]DFP, was not eliminated by this experiment. This band might correspond to an associated protein or an endogenous protease inhibitor of NP (Fig. 6, *A–D*).

Characterization of Brain NP—The characteristics of enzyme activity of brain NP were identical to those of r-NP (Table I). The K_m values were very similar between brain NP and r-NP, suggesting that these molecules are enzymatically identical (Tables I and IV). As shown in Table I, brain NP had a lower specific activity than r-NP, which was thought to be due to the presence of the NP binding protein that inhibits the amidolytic activity of NP in the partially purified brain extracts. The partially purified brain NP was itself enzymatically active (Table I). The highest NP activity was found against Boc-Val-Pro-Arg-MCA (Table I). Synthetic substrates were preferentially cleaved by the enzyme at an Arg or Lys residue at the P1 position (Table I). Thus, enzyme characterization studies of r-NP and NP clearly demonstrated that the protease is a novel trypsin-type serine protease existing as a naturally active enzyme (Tables I and IV).

Subcellular Localization of Brain NP in the Hippocampus—To define the distribution of endogenous brain NP in various subcellular compartments, the mouse brain homogenate was fractionated, as illustrated in Fig. 7*A*, followed by immunoprecipitation and immunoblotting analysis. Major and a minor weak bands corresponding to brain NP and its degradation product, respectively, were detected in the soluble fraction (*A*), whereas no band was detected in the Triton X-100-soluble fraction (*B* and *C*). A faint band of brain NP was also detectable in the cytoskeleton-rich fraction (*D*).

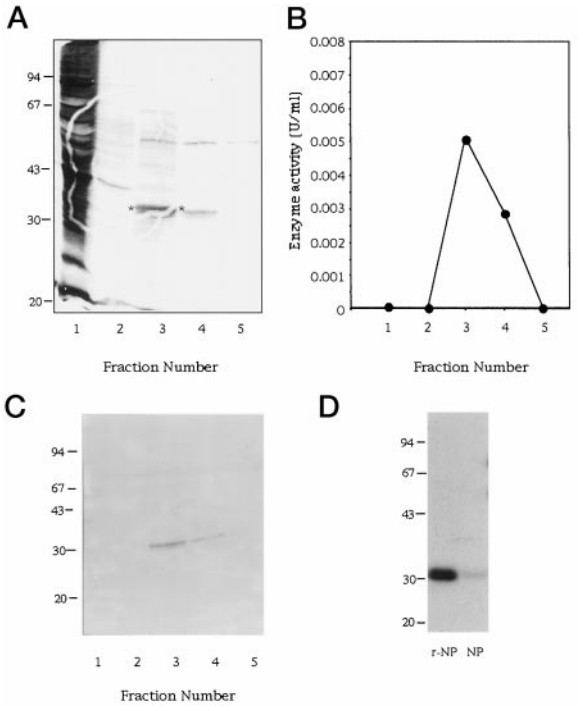

FIG. 6. **Partial purification of NP.** The mAbB5-coupled affinity gel (see "Experimental Procedures") was used for purification of NP from brain. Fraction size was 1 ml each. *A*, electrophoresis of aliquots (10 μl) of eluates was performed in a 12.5% gel followed by silver staining and Western blotting. *Lane 1*, eluate fraction; *lane 2*, pool of wash; and *lanes 3–5*, eluted 1-ml fractions. *B*, enzyme activity of each fraction measured by Boc-Val-Pro-Arg-MCA as a substrate. Note that cleavage activity for the chromogenic substrate was found in fractions 3 and 4. *C*, Western blotting analysis of each fraction demonstrated that NP was present in fractions 3 and 4. *D*, autoradiography of [^{3}H]DFP bound to partially purified NP and r-NP. A single band of approximately 32 kDa was detected by [^{3}H]DFP autoradiography. Aliquots of 10 μl of partially purified brain NP (*NP*, fraction 3) and 2 ng of r-NP were electrophoresed.

TABLE IV
Comparison of K_m values between brain NP and r-NP

Substrate	r-NP	brain NP
Boc-Val-Pro-Arg MCA	270 (μM)	300 (μM)
Boc-Phe-Ser-Arg-MCA	500	540
D-Val-Leu-Arg-pNA	230	280
Boc-Asp-Pro-Arg-MCA	398	—[a]

[a] —, not tested.

DISCUSSION

It has been suggested that neural plasticity is based on the actions of a variety of proteases and their inhibitors (3, 22–25). Various neurological stimuli induce tissue-type plasminogen activator (tPA) mRNA in the brain, and it has been shown to be involved in seizures, kindling, and neural degeneration (5, 23, 26). It was also suggested that tPA might be related to repulsion of neural outgrowth, because inhibitors of tPA increase neurite outgrowth in sympathetic ganglion cells (27). Such induction of neurite retraction on the cultured central and peripheral neurons was also found for thrombin (4, 28–31). However, these proteases have been shown to be involved only in glial to neuronal interactions in the developing brain (1, 5,

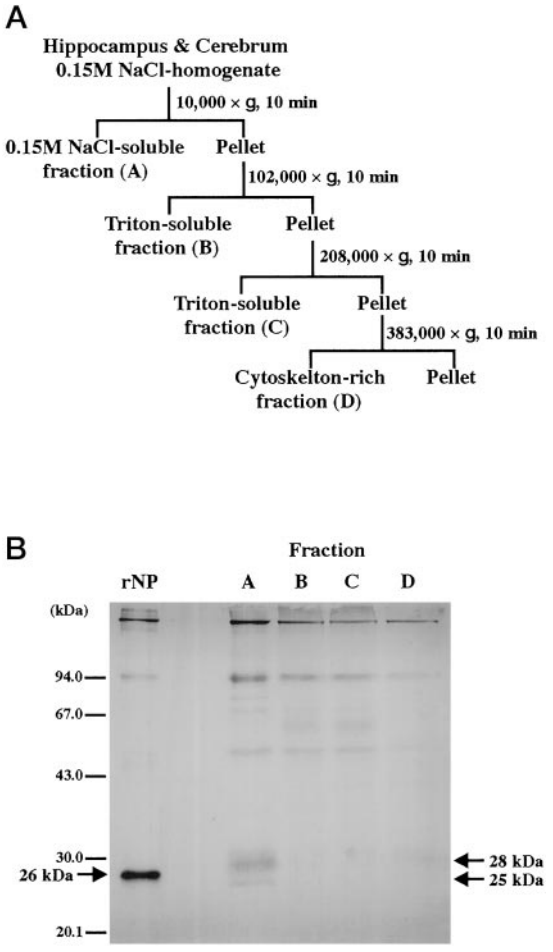

FIG. 7. **Subcellular fractionation of brain NP.** *A*, schematic illustration of tissue extraction used in the present study. A detailed description and protocol is provided under "Experimental Procedures." *B*, a major band and a weak minor band of brain NP were detectable at approximately 28 and 25 kDa in the buffered saline-soluble fraction (*lane A*). A faint band of brain NP was also detectable in the cytoskeleton-rich fraction (*lane D*). Molecular weight standards are indicated in the *left margin*. The r-NP was electrophoresed at 26 kDa under nonreducing conditions.

24). On the other hand, proteases relating to intersynaptic connections among neurons to neurons in the matured brain have not been identified. We hypothesized the existence of a novel protease localized in and released from the pyramidal neurons of the hippocampus, and we cloned the NP cDNA from these brain areas as described in our previous reports (8, 9, 32). The NP mRNA was expressed in pyramidal neurons of the hippocampus with the highest density in the brain, and the neural responses of this gene strongly suggested that this protease has important physiological functions in the limbic brain.

Analyses of the deduced amino acid sequence of the NP3 cDNA suggested that this protein has protease activity. Studies were begun to produce a recombinant protein in the baculovirus-insect cell system and to measure the protease activity of the recombinant protein. However, in contrast to our initial assumption, the recombinant protein did not show clear cleavage activity for any synthetic protease substrates examined. The present study, however, clearly demonstrated that recombinant prototype NP (r-pro-NP) secreted from insect cells was processed by endoproteases and was converted to the enzymatically active form (r-NP) as shown in Fig. 4. It is interesting that the activational processing was brought about by the removal of only four N-terminal amino acids.

Brain NP which was affinity purified from brain homogenate had enzymatic properties identical to those of r-NP. The enzyme preferentially hydrolyzes Arg-*X* bonds and, to a lesser extent, Lys-*X* bonds. In addition, the tripeptide MCA substrate Z-Pro-Phe-Arg-MCA, but not the dipeptide MCA substrate Z-Phe-Arg-MCA, was cleaved by the enzyme, and thus at least four binding sites (S_3, S_2, S_1, and S_1') seem to be a prerequisite for hydrolysis (33, 34). The enzyme therefore appears to contain multiple amino acid side chain binding sites in its active site. The S_3 subsite appears to favor hydrophobic (Val, Phe) side chains, judging from the higher specific activities of NP for Boc-Val-Pro-Arg-MCA and Boc-Phe-Ser-Arg-MCA than for Boc-Asp-Pro-Arg-MCA (see Table I). The order of specific activities of the three highest activity substrates was Boc-Val-Pro-Arg-MCA > Boc-Phe-Ser-Arg-MCA > D-Val-Leu-Arg-pNA (see Table I). Human thrombin cleaved Boc-Val-Pro-Arg-MCA faster than Boc-Phe-Ser-Arg-MCA, but the activity for the latter substrate was only 3% of that for the former (*cf.* 48–78% in NP, Table I) (35). In addition, porcine kallikrein and plasmin cleaved Boc-Val-Pro-Arg-MCA more slowly than D-Val-Leu-Arg-pNA (35). Thus, the substrate specificity of NP is very different from those of thrombin, tissue kallikrein, and plasmin.

By the subcellular fractionation of mouse brain, NP co-fractionated with the saline-soluble fraction which is composed of cytoplasm and extracellular soluble components (Fig. 7 and Ref. 15). As the hydrophobic signal sequence is encoded in the NP3 cDNA (8) and the recombinant protein is released into medium from NP3 cDNA-infected insect cells as shown in the present study and NP3 cDNA-transfected neuroblastoma cells (Neuro 2a).[2] Therefore, NP is strongly suggested to be an extracellular protease. Recently, we reported that intraventricular injection of monoclonal antibodies specific to NP into mouse brain reduced the epileptic pattern of electroencephalograms and epileptic behavior (11). As exogenously applied antibodies can hardly pass across the plasma membrane into living cells, the antibodies are thought to modify the activity of extracellular NP. Taken together, these observations suggested that brain NP secreted from hippocampal pyramidal neurons as a zymogen and undergone an activational processing might be involved in neural plasticity-related protease function (present study and Refs. 8, 9, and 11).

Since NP is considered to be a secretory serine protease as described above, the extracellular matrix molecules are good candidates for the physiological substrates of NP. r-NP effectively cleaved fibronectin which is a major extracellular matrix protein expressed in the nervous system (present study and Ref. 37). The specific cleavage by r-NP as shown in the present study might directly affect fibronectin's functions as a cell adhesion molecule, because the N-terminal 5 FnI domains contain the main fibrin-binding site (21). Such cleavage pattern of fibronectin by r-NP is analogous to that by plasmin but was different from those by thrombin, plasminogen activator, and trypsin (19, 38).

In conclusion, the present study clearly demonstrated characters of r-NP and brain NP as a novel serine protease and also presented that the protease might be involved in neural plasticity by potential modification of the extracellular environments.

Acknowledgments—We thank Drs. Fang-Sik Che of NAIST and Takeshi Kato of Yokohama City University for their suggestions on protein sequence analysis and activational processing of zymogen, respectively. We also thank Junko Tsukamoto for performing TOFMS.

[2] T. Oka, Y. Hashimoto, S. Shiosaka, and K. Kato, unpublished observations.

REFERENCES

1. Monard, D. (1988) *Trends Neurosci.* **11,** 541–544
2. Pittman, R. N., Ivans, J. K., and Buettner, H. M. (1989) *J. Neurosci.* **9,** 4269–4286
3. Liu, Y., Field, R. D., Fitzgerald, S., Festoff, B. W., and Nelson, P. G. (1993) *J. Neurobiol.* **25,** 325–335
4. Suiden, H. S., Stone, S. R., Hemmings, B. A., and Monard, D. (1992) *Neuron* **8,** 363–375
5. Tsirka, S. E., Gualandris, A., Amaral, D. G., and Strickland, S. (1995) *Nature* **377,** 340–344
6. Dent, M. A. R., Sumi, Y., Morris, R. J., and Seeley, P. J. (1993) *Eur. J. Neurosci.* **5,** 633–647
7. Rao, J. S., Sawana, R., Gokaslan, Z. L., Yung, W. K. A., Goldstein, G. W., and Laterra, J. (1996) *J. Neurochem.* **66,** 1657–1664
8. Chen, Z.-L., Yoshida, S., Kato, K., Momota, Y., Suzuki, J., Tanaka, T., Ito, J., Nishino, H., Aimoto, S., Kiyama, H., and Shiosaka, S. (1995) *J. Neurosci.* **15,** 5088–5097
9. Okabe, A., Momota, Y., Yoshida, S., Hirata, A., Ito, J., Nishino, H., and Shiosaka, S. (1996) *Brain Res.* **728,** 116–120
10. Nishizawa, K., Yano, T., Shibata, M., Ando, S., Saga, S., Takahashi, T., and Inagaki, M. (1991) *J. Biol. Chem.* **266,** 3074–3079
11. Momota, Y., Yoshida, S., Ito, J., Shibata, M., Kato, K., Sakurai, K., Matsumoto, K., and Shiosaka, S. (1997) *Eur. J. Neurosci.* **10,** 760–764
12. Laemmli, U. K. (1970) *Nature* **227,** 680–685
13. Dammerval, C., Le Guilloux, M., Blaisonneau, J., and de Vienne, D. (1987) *Electrophoresis* **8,** 158–159
14. Wiechelman, K., Braun, R., and Fitzpatrick, J. (1988) *Anal. Biochem.* **175,** 231–237
15. Yen, S.-H., Kenessey, A., Lee, S. C., and Dickson, D. W. (1995) *J. Neurochem.* **65,** 2577–2584
16. Kyte, J., and Doolittle, R. F. (1982) *J. Mol. Biol.* **157,** 105–132
17. Vu, T. K., Hung, D. T., Wheaton, V. I., and Coughin, S. R. (1991) *Cell* **64,** 1057–1068
18. Rasmussen, U. B., Gachet, C., Schlesinger, Y., Hanau, D., Uhlmann, P., Van Obberghen-Schilling, E., Pouyssegur, J., Cazenave, J. P., and Pavirani, A. (1993) *J. Biol. Chem.* **268,** 14322–14328
19. Quigley, J. P., Gold, L. I., Schwimmer, R., and Sullivan, L. M. (1987) *Proc. Natl. Acad. Sci. U. S. A.* **84,** 2776–2780
20. Furie, M., and Rifkin, D. B. (1980) *J. Biol. Chem.* **255,** 3134–3140
21. Chothia, C., and Jones, E. Y. (1997) *Annu. Rev. Biochem.* **66,** 823–862
22. Lynch, G., and Baudry, M. (1984) *Science* **224,** 1067–1063
23. Qian, Z., Gilbert, M. E., Colicos, M. A., Kandel, E. R., and Kuhl, D. (1993) *Nature* **361,** 453–457
24. Nelson, P. G., Fields, R. D., and Lie, Y. (1994) *Perspect. Dev. Neurobiol.* **2,** 399–407
25. Frey, U., Müller, M., and Kuhl, D. (1996) *J. Neurosci.* **15,** 2057–2063
26. Twining, S. S. (1994) *Crit. Rev. Biochem. Mol. Biol.* **29,** 315–383
27. Seeds, N. W., Friedman, G., Hayden, S., Thewke, D., Haffke, S., McGuire, P., and Krystosek, A. (1996) *Semin. Neurosci.* **8,** 405–412
28. Jalink, K., and Moolenaar, W. J. (1992) *J. Cell Biol.* **118,** 411–419
29. Gurwitz, D., and Cunningham, D. D. (1988) *Proc. Natl. Acad. Sci. U. S. A.* **85,** 3440–3444
30. Hawkins, R. L., and Seeds, N. W. (1886) *Brain Res.* **398,** 63–70
31. Grand, R. J. A., Grabham, P. W., Gallimore, M. J., and Gallimore, P. H. (1989) *EMBO J.* **8,** 2209–2215
32. Suzuki, J., Yoshida, S., Chen, Z.-L., Momota, Y., Kato, K., Hirata, A., and Shiosaka, S. (1995) *Neurosci. Res.* **23,** 345–351
33. Schechter, I., and Berger, A. (1967) *Biochem. Biophys. Res. Commun.* **27,** 157–162
34. Schechter, I., and Berger, A. (1968) *Biochem. Biophys. Res. Commun.* **32,** 898–902
35. Uchino, T., Sakurai, Y., Nishigai, M., Takahashi, T., Arakawa, H., Ikai, A., and Takahashi, K. (1993) *J. Biol. Chem.* **268,** 527–533
36. Chen, Z.-L., Momota, Y., Kato, K., Taniguchi, M., Inoue, N., Shiosaka, S., and Yoshida, S. (1997) *J. Histochem. Cytochem.* **46,** 313–320
37. Sanes, J. R. (1983) *Annu. Rev. Physiol.* **45,** 581–600
38. Pierschbacher, M. D., Hayman, E. G., and Ruoslahti, E. (1981) *Cell* **26,** 259–267